Experimental study of the effects of vent geometry on the dispersion of a buoyant gas in a small enclosure

B. Cariteau, I. Tkatschenko

C.E.A. Saclay, D.E.N., D.M.2S., S.F.M.E, Laboratoire d'Etude Expérimentale des Fluides, 91191 Gif sur Yvette cedex, FRANCE

Phone: +33 (0)1.69.08.24.71, Fax: +33 (0)1.69.08.82.29

e-mail : benjamin.cariteau@cea.fr (Corresponding author)

Abstract : We present an experimental study on the dispersion of helium in an enclosure of $1m^3$ with natural ventilation through one vent. Three vent geometries have been studied. Injection parameters have been varied so that the injection Richardson number ranges from $2\ 10^{-6}$ to 9 and the volume Richardson number, which gives the ability of the release to mix the enclosure content ranges from $8\ 10^{-4}$ to 900. It is found that the vertical distribution of helium volume fraction can exhibit significant gradient. Nevertheless, the results are compared to the simple analytical model based on the homogenous mixture hypothesis which gives fairly good estimate of the maximum helium volume fraction.

1. INTRODUCTION

As part of safety studies related to the use of hydrogen in confined environment, it is of primary importance to have a good knowledge of the dispersion mechanisms of this low density gas in air during a release characteristic of a leak. Studies on the dispersion of buoyant jet in enclosures without ventilation date back to the late sixties [1] with applications on geophysical flow and continue during the last thirty years in various fields such as filling liquid natural gas tank [2] or safety analysis for the domestic use of natural gas [3]. More recently experiments on the dispersion of helium in a large scale enclosure ($40m^3$) have been conducted [4]. In a companion paper [5] we present an experimental study of the various regimes encountered in the dispersion of a buoyant jet in a $1m^3$ enclosure for a wide range of injection condition. The influence of a small ventilation of the enclosure has also been study both with experimental and numerical approaches [6], [7]. Indeed, beyond these fundamental aspects, the influence of natural ventilation through one or more vents is the logical next step. Of course, final hydrogen based system have such openings. Natural ventilation dramatically changes the dispersion properties. Linden, Lane-Serff and Smeed [8] have investigated in details natural ventilation through one or two vents based on experiments in salt water. They proposed for each situation a simple analytic model. Linden [9] gives a review in the context of thermal effects in naturally ventilated rooms. Efficient numerical modeling for safety studies is a major issue that leads to constant efforts for its development together with experimental validation in more or less simplified situations (see *e.g.* [10], [11], [12] [13] and [14]). Whatever the amount of experimental studies, there is still a need of new data due to the wide range of possible scenarii.

In a previous study [4], we investigate the influence of one vent on the dispersion of helium in an enclosure of $40m^3$. These experiments were conducted for low flow rate release, *i.e.*, the injection flow is close to a pure plume. These experiments show the persistence of a vertical gradient in the distribution of helium volume fraction. An accidental hydrogen leak may occur in the hydrogen system which size can be of the order of $1m^3$. In such a small volume, inertial effects of a buoyant jet of high velocity must have a strong influence on the mixing and dispersion. Experiments have been conducted on a $1m^3$ enclosure without natural ventilation [5]. From the results we obtain the injection conditions that lead to a homogeneous dispersion over the entire volume of the enclosure and related then to a correlation derived by Cleaver, Marshall and Linden [3]. In the present study we investigate

the influence of one vent located near the ceiling of the $1m^3$ enclosure. The focuses are high injection velocity and vent geometry influences. More precisely, some questions are addressed here. For a plume-like injection in such a small volume, is the vertical distribution stratified of homogeneous? When the injection is jet-like, is there still formation of a homogeneous layer of increasing thickness with jet velocity and is the criteria for a homogeneous dispersion still valid? What is the vent geometry influence? And, is the model derived by Linden *et. al.* [8] applicable?

In the following, previous results and analytic modeling considerations are reviewed in section 2. Section 3 is devoted to the presentation of the experimental setup. The results are discussed in section 4 and the conclusions are given in section 5.

2. REVIEW OF PREVIOUS RESULTS

We consider here the case of helium injection in an enclosure initially filled with air. Thermal effects are neglected and the pressure in the enclosure is supposed constant. The source is vertical and oriented upward. It is characterized by the density of helium ρ_0, its volume flow rate Q_0 and horizontal cross section $S_0=\pi R_0^2$. The average source velocity U_0, is deduced from the last two parameters. The various injection flow regimes are characterized by the injection Richardson number:

$$Ri_0 = g\frac{\rho_a - \rho_0}{\rho_0}\frac{R_0}{U_0^2} \tag{1}$$

where ρ_a is air density.

In a companion paper [5] it has been verified that volume Richardson number introduced by Cleaver *et. al.* [3], is the relevant parameter that will characterize the filling regime, *i.e.*, stratified, stratified with a homogeneous layer or homogeneous. This Richardson number is based on a characteristic length scale of the enclosure. Here, the volume V is chosen to obtain this length scale :

$$Ri_v = g\frac{\rho_a - \rho_0}{\rho_0}\frac{V^{1/3}}{U_0^2}, \tag{2}$$

Cleaver *et. al.* [3] propose an empirical correlation to estimate the thickness d of the homogeneous layer:

$$\frac{d}{R_0} = \frac{C_i}{\sqrt{Ri_v}}. \tag{3}$$

where C_i is a constant depending on the orientation of the source. For a vertical upward source, it has been measured at 25. This correlation have been found to be in a fairly good accordance with the experimental results obtained on a $1m^3$ enclosure with helium injection [5], provided that the volume Richardson number is lower than 0.01. For volume Richardson number ranging from 0.01 to 1, a homogeneous layer still exists but its thickness is under-estimated by the correlation (3). For values higher than 1, there is no more homogenous layer.

The use of the correlation (3) as a criterion for complete homogenization during the filling is also in good accordance with experimental results (see [5]), so that the condition to reach this regime is:

$$Ri_v < \left(\frac{25R_0}{H}\right)^2. \tag{4}$$

with H the height of the enclosure. The validity of this criterion has only been verified for vertical upward source.

These considerations concern enclosures without ventilation. In the present study we investigate the effect of a vent located near the ceiling of the enclosure, thus producing natural ventilation of the enclosure. Linden, Lane-Serff and Smeed [8] propose a simple analytical model of ventilation with one vent. For this model, the source produces a plume of buoyancy flux:

$$B_0 = g\frac{\rho_a - \rho_0}{\rho_a}Q_0 = g_0' Q_0 \tag{5}$$

where g is the gravity acceleration and g_0' is the source reduced gravity. The vent geometry is defined by its vertical extension h and surface S. It is located near the ceiling. The flow across the vent is driven only by buoyancy. The incoming fresh air is supposed to mix the enclosure content so that the density in the enclosure is considered homogeneous. For convenience, the model proposed by Linden *et. al.* [8] is rewritten in terms of helium volume fraction. Considering a constant pressure equal to the atmospheric pressure and constant temperature, the helium volume fraction is related to the density ρ of the mixture by:

$$X = \frac{\rho_a - \rho}{\rho_a - \rho_0}. \tag{6}$$

The exchange volume flow rate through the vent only depends on the density difference between the enclosure and the exterior:

$$Q_e = C_D S (X g_0' h)^{1/2}. \tag{7}$$

where C_D is a discharge coefficient equal to 0.25 [9]. The equation for time variation of the volume fraction in the enclosure comes from the mass conservation:

$$\frac{dX}{dt} = \frac{Q_0}{V} - \frac{C_D S (g_0' h)^{1/2}}{V} X^{3/2}, \tag{8}$$

With an initial volume fraction to zero and a constant source volume flow rate, the evolution of the volume fraction in the enclosure reaches a steady state. The final volume fraction is then given by:

$$X_f = \left[\frac{Q_0}{C_D S (g_0' h)^{1/2}} \right]^{2/3} \tag{9}$$

The characteristic time of the transient is given by:

$$\tau = \frac{2V}{C_D S} \left(g_f' h \right)^{-1/2}, \tag{10}$$

where g'_f is the final reduced gravity in the enclosure associated with the steady state density of the mixture in the enclosure ρ_f:

$$g_f' = g \frac{\rho_a - \rho_f}{\rho_a}. \tag{11}$$

3. EXPERIMENTAL SETUP AND CONDITIONS

The enclosure is a parallelepiped with a square base of 0.93x0.93m^2 and 1.26m high (see Fig. 1). The vent is located on a side wall, near the ceiling. Three different rectangular vents have been tested. The larger is 90cm wide and 18cm high (referred as (a) in the following). Its surface is 1620cm^2. The two other are approximately of the same surface. One is a square of 18x18cm^2 (referred as (b)) and the second is 90x3.5cm^2 (referred as (c)). Their surfaces are 325cm^2 and 315cm^2, respectively.

Helium is injected from the bottom of the enclosure through a tube of 5mm or 20mm in diameter, centered in the horizontal section and directed upward. The outlet of the injection tube is at 21cm from the bottom.

Injections were performed with two mass flow controllers chosen according to the desired flow rate. One regulator has a 20Nl/min full scale and the other has a 350Nl/min full scale. The error on the mass flow rate for the 20Nl/min controller is 0.1% of full scale plus 0.5% of the set point. For 350Nl/min controller, the error on the mass flow rate is 0.2% of full scale plus 0.7% of the set point.

The range of tested flow rates is 1Nl/min to 300Nl/min. With pure helium and the 5mm diameter source, this leads to a injection Richardson number ranging from 0.2 to 2 10^{-6}, and a volume Richardson number ranging from 75 to 8 10^{-4}. With the 20mm diameter source, the lowest tested flow rate is 5Nl/min. The injection Richardson number varies from 7 to 0.003 and the volume Richardson number from 740 to 0.2.

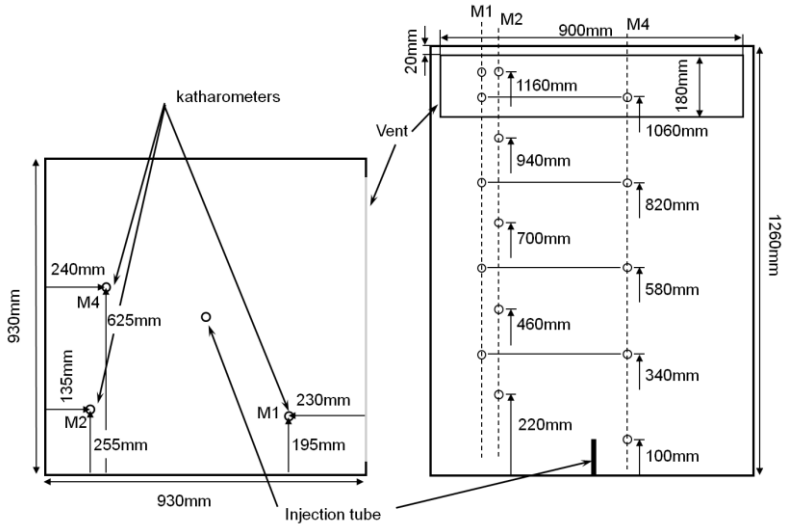

Figure 1 : Experimental setup scheme, top view on the left and side view on the write.

The helium volume fraction is measured with min-katharometers distributed along three vertical lines as shown on Fig.1 (see *e.g.* [4] for a detailed descriptions of mini-kathrometers). They are placed as far as possible from the source and walls, where the volume fraction distribution is supposed to be at least independent on the horizontal position. The sensors on lines M2 and M4 are distributed on different vertical position so that this assumption may be checked. Along the third line, the sensors are distributed in order to estimate the possible horizontal variations. Measurements of the 15 sensors are simultaneously sampled with a period of 5s. Temperature in the enclosure is measured with a thermocouple.

4. RESULTS

Prior to discuss in detailed the results obtained, Fig. 2 shows typical time records of the helium volume fraction during two releases tests with the 5mm source at a flow rate of 100Nl/min, one with vent (a) and the other with vent (b). The different curved on these graphs correspond to sensors at different horizontal location and at the same altitude. The general evolution is characterized by a transient increase of the helium volume fraction at all height. After this, a steady state is reached. However, the records during the steady state exhibit small amplitude perturbations probably due to inhomogeneity in turbulent mixing and also to gravity waves that may propagate in a clearly vertically stratified environment. Thus, in the following, when discussing about the results in steady state regime, the data are time averaged to avoid the influence of these perturbations.

From these graphs (Fig. 2), the horizontal variation of the helium volume fraction away from the source can be evaluated. It comes that with the smallest vent (b), there are clearly no horizontal dependency of the volume fraction. Even the fluctuations are in close correlation between the two horizontal positions of the sensors. This suggests that the fluctuations in that case are due to wave propagation rather than turbulence.

With the largest vent (a) some difference are visible, mainly on the highest sensors. The volume fraction near the vent is slightly lower than that measured on the other side of the enclosure. There are only two measurement locations in the horizontal cross section so we cannot conclude strictly about the overall horizontal variations. But, since the vent surface is very large, about 20% of the horizontal cross section, and due to the proximity of the sensor and the vent, we can suppose that this diminution of the volume fraction can be a local effect of the incoming air. This assumption may be reinforced by the vanishing difference between the measurements at the two horizontal positions for sensors in the lower part of the enclosure. In the following subsections, we will neglect this decrease of the volume fraction near the largest vent and consider that the vertical variations given by the two vertical lines M2 and M4 is representative of the distribution in a large part of the enclosure volume.

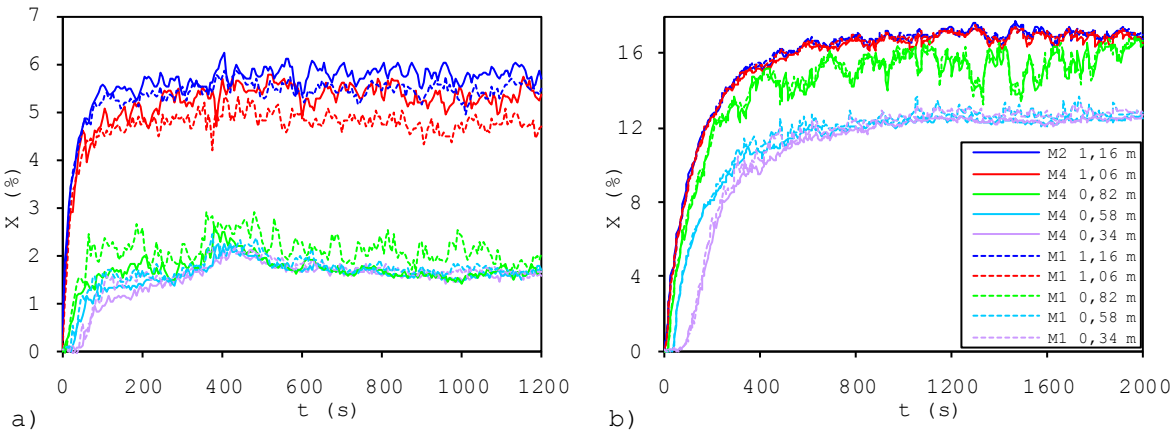

Figure 2: Temporal variations of helium volume fraction during injection with the 20mm source at 40Nl/min; a) with vent (a) and b) with vent (b).

4.1. The steady state regime

As previously mentioned, the data presented in this subsection results from a time average of the measured volume fraction after the transient. The vertical variations of the helium volume fraction are obtained from the two sensors lines M2 and M4. Form the vertical profiles, the helium volume fraction spatial average is obtained by numerical integration using the classical trapezoid method. In the following, the spatial average of the volume fraction is noted as, <X>.

Vertical profiles for Ri_v>>1:

High values of the volume Richardson number are mainly achieved with the 20mm source for flow rates ranging from 5 to 100Nl/min. In Fig. 3, the profiles of volume fraction of helium in these conditions are almost self-similar. Profiles for each vent exhibit some common characteristics. From the top to bottom of the enclosure, one finds successively, a layer more or less homogeneous, below which a steep gradient takes place, and again a homogeneous layer. Depending on the vent, these areas are characterized by different thickness, volume fraction and gradient. The result obtained with the vent (c) has in addition a fourth zone near the bottom up to 0.27H where the volume fraction strongly decreases.

With the vent (a), the top homogeneous area is weakly apparent with a helium volume fraction around 2<X> and a thickness less than 0.2H. With the vent (b), this area appears clearly. The volume fraction of helium is then of 1.15<X> and its height is 0.3H. For the vent (c), the volume fraction in the top homogeneous layer and its height is similar to that obtained with the vent (b).

The layer of strong volume fraction variation presents a maximum gradient value with the vent (a). It is 6.5<X>/H, over a height of 0.2H. The gradient decreased to 1.5<X>/H for the vent (b) over a similar height. It becomes small for the vent (c) with 0.5<X>/H and a height of 0.1H.

The helium volume fraction in the bottom homogeneous layer is about 0.63<X>, 0.87<X> and <X>, for vents (a), (b) and (c), respectively. The homogeneity of this layer is weaker for the vent (c), for which there is a small gradient of 0.3<X>/H between z=0.3H and z=0.65H.

These results show that the flow of air entering through the vent and the subsequent conjectured recirculation in the enclosure does not lead to a homogeneous mixture throughout the height of the enclosure. The capacity of this air flow to homogenize the mixture depends on the surface of the vent and height but there is still a layer of volume fraction above the average in the upper part of the enclosure. Ultimately, with the vent (c) whose height is very low, the air seems to drop straight to the bottom of the chamber to form a highly diluted layer of low thickness.

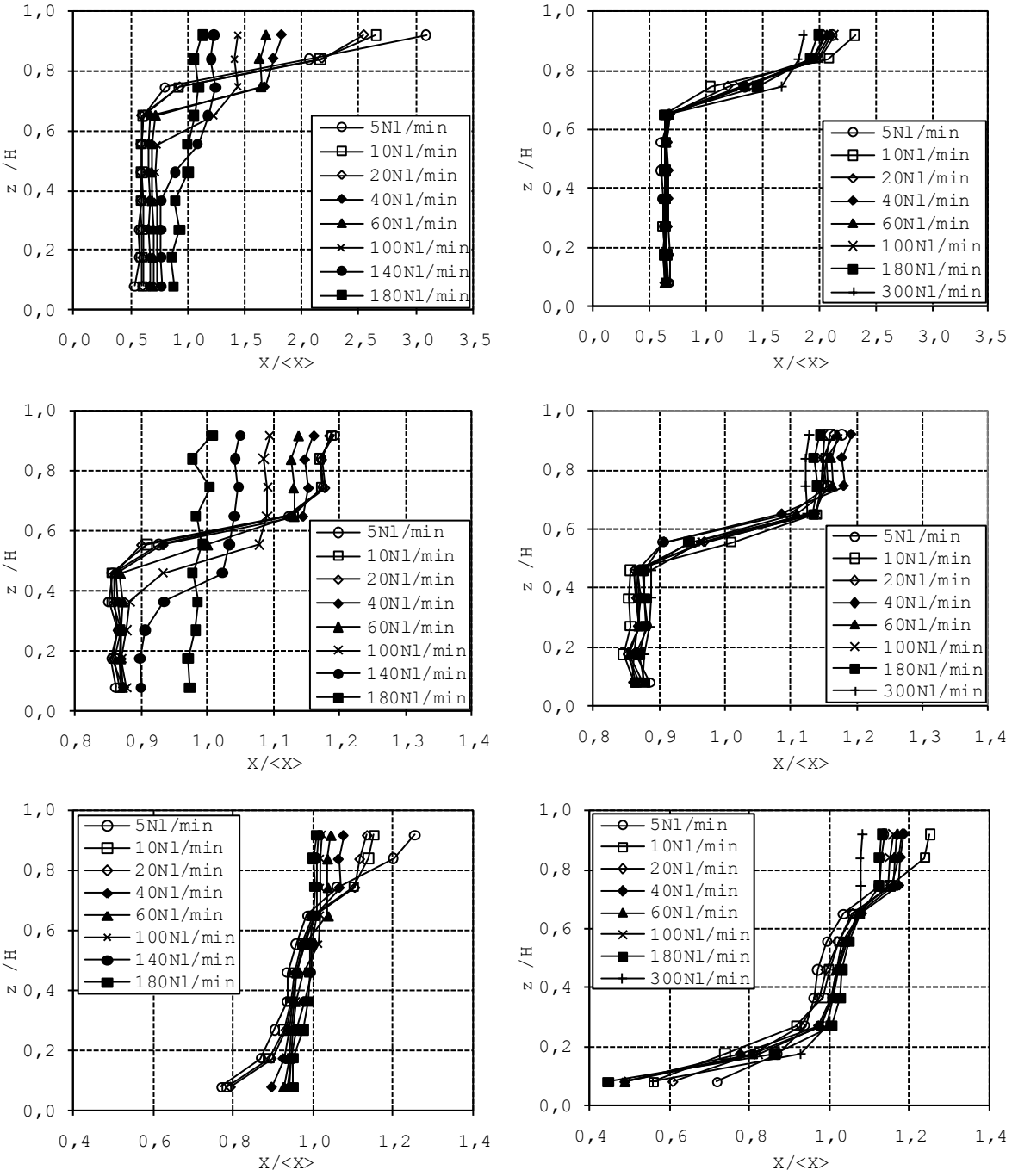

Figure 3 : Steady state vertical distribution of the volume fraction, with the 5mm source (left column) and 20mm source (write column), for each vent (a), (b) and (c) from the top to the bottom.

Vertical profiles for Ri_v<<1:

In the limit of very small volume Richardson number reached with the 5mm source and the highest flow rate, we find the homogeneous regime observed in experiment without vent (see [5]). The homogeneous filling regime is obtained whatever the vent geometry. The critical value of the volume Richardson number to reach this regime is measured at 0.0023 (*i.e.* at a flow rate of 180Nl/min). This is precisely the same value as in the case of the enclosure without vent. Thus, the presence of a vent does not alter the criterion of uniform filling.

As the volume Richardson number increases, the volume fraction profiles present stratification. The overall volume fraction gradient increases for volume Richardson number values ranging from 0.002 to 0.05 (to be 140Nl/min 40Nl/min).

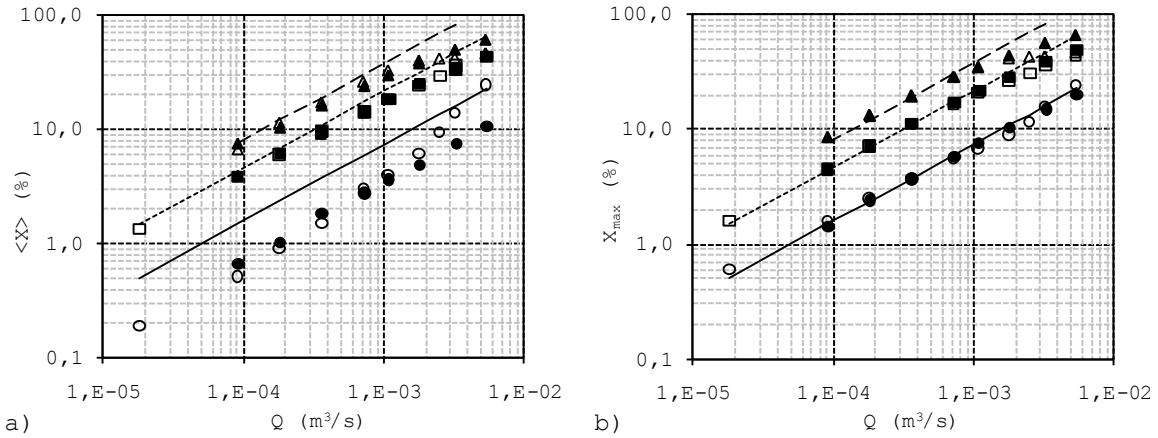

Figure 4 : Steady state helium volume fraction, average (a) and maximum (b), as a function of the injection volume flow rate for vent (a) (circles), (b) (squares) and (c) (triangles). Filled symbols correspond to the 20mm source and empty symbols for the 5mm source. Lines represent the model eq.(9) with a discharge coefficient of 0.25 for each vent, (a) (continuous), (b) (short dashed line) and (c) (long dashed line).

With the vent (b), there is clearly the formation of a homogeneous layer in the upper part whose thickness decreases as the Richardson number density increases. This homogeneous layer and its thickness variation are less marked on the results obtained with the vents of large width ((a) and (c)).

For volume Richardson numbers higher than 0.05 (*i.e.* for flow rate lower than 40Nl/min), one recovers profiles similar to those obtained with the 20mm source. In particular, with the vents (a) and (b), the profiles are self-similarity as observed for large values of the volume Richardson number. With the vent (c), the interpretations are made more difficult due to weak vertical variations, but this trend also seems to be emerging.

To summarize, these measures show that the volume fraction vertical variations near the ceiling are clearly strongly influenced by the presence of a vent. The results obtained for low values of the volume Richardson number show that the inertial effects due to the source does not become visible if its value is less than 0.05. Between this value and 1, inertial effects leading to overturning are masked by the effects related to the presence of the vent.

Variations of the spatial average volume fraction with the flow rate:

The evolution of the average helium volume fraction in steady state regime as a function of the source flow rate is shown in Fig. 4a for each vent. The measurements are compared to the homogeneous model given by eq. (9) with a discharge coefficient C_D of 0.25.

Whatever the geometry of the vent, the average helium volume fraction well follows the power law $Q^{2/3}$ for an injection rate of less than $0.001 m^3/s$ (about 60Nl/min at 20°C). With the vents (b) and (c), the value given by the model is very close to experimental results. This is not the case for the results obtained with the vent (a) that the model significantly overestimates. Beyond a rate of $0.001 m^3/s$, the results clearly differ from the power law $Q^{2/3}$ with the exception of those obtained with the vent (a) and the source of 20mm diameter. On the graph of Fig. 4b the maximum helium volume fraction, recorded near the ceiling, is plotted against the flow rate. The results are generally closer to the homogeneous model. This is particularly noticeable with the results for the vent (a).

The analytical model is based on the assumption that flow through the vent is driven solely by the density difference between inside and outside the enclosure. Also the distribution of helium in the enclosure is supposed homogeneous. As we have shown on the vertical profiles, the distribution is not uniform in the chamber. This may explained that the results are closer to the model when considering the actual volume fraction of helium at the level of the vent.

Beyond the flow rate of $0.001 m^3/s$, deviations from the model suggest that the outflow is no longer imposed by the density difference solely. Results on Fig. 4b show that this transition is independent of the diameter of the source with the vents (b) and (c).

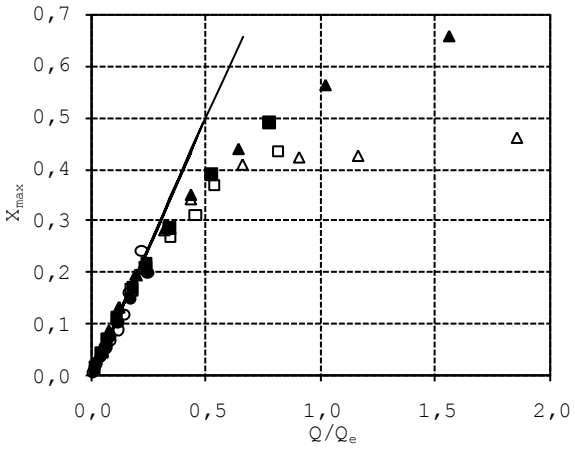

Figure 5: Steady state maximum helium volume fraction as a function of the ratio of the injection volume flow rate to the exit flow rate calculated from eq.(7). The line correspond to the model given by eq.(9). The symbols legend is the same than Fig. 4.

Moreover, it does not appear in the case of the vent (a). This leads to the conclusion that the volume Richardson number may not be the relevant parameter that defines this transition.

On the graph in Fig. 5, the maximum volume fraction of helium is plotted against the ratio Q_0/Q_e between the source volume flow rate and the exchange volume flow rate through the vent estimated with eq. (7). The measured maximum volume fraction is used for the evaluation of the exchange flow rate. If the exchange rate results only from the density difference then, the volume fraction at the vent is equal to Q_0/Q_e. This corresponds to the continuous line on the graph in Fig. 5. As a consequence, for purely gravity driven flow, Q_0/Q_e must rely below 1. But this is not the case, which clearly indicates the existence of an additional contribution in the outflow of the enclosure. For values of this ratio below 0.3, all data follow the straight line corresponding to the model. Note that the results for the vent (a) give a flow rate ratio below 0.3 for the range of source flow rate. Beyond this value, some additional pressure effects lead to a deviation from the model.

The contribution of the pressure may be due to inertial effects of the jet. This is clearly the case for values of Q_0/Q_e higher than 0.6 since the volume fraction is significantly lower when the source diameter decreases for the same flow rate. That is to say, the volume Richardson number has a significant influence. For values of Q_0/Q_e between 0.3 and 0.6, the differences observed for different source diameters at a constant flow rate are small. In that case, the volume Richardson number has a little influence. However, the maximum volume fraction already much lower than expected in the absence of pressure effects. There remains therefore a significant pressure effect but it seems more related to the volume flux than to the inertial effects of the source. Thus, even for a high Richardson numbers, this pressure effect is likely to occur if the surface of the vent is too small.

4.2. The transient regime

In this subsection, we first discuss the time evolution of the average helium volume fraction during the transient. The vertical profile at each recorded time is integrated to obtain the spatial average of the volume fraction. The results show on Fig. 7 for each vent and injection conditions are compared to the numerical integration of eq. (8). All the data are normalized by the measured steady state volume fraction. The time is normalized with the characteristic value given by eq. (10).

The transient time is experimentally defined as the time needed to reach 90% of the steady state volume fraction. It varies between 0.5τ and τ except for the injection with the 5mm source at 5Nl/min and vent (c) for which the transient takes 2τ. It seems that some perturbation have affected this measure (strong thermal variation in the experimental hall, air draft, for instance).

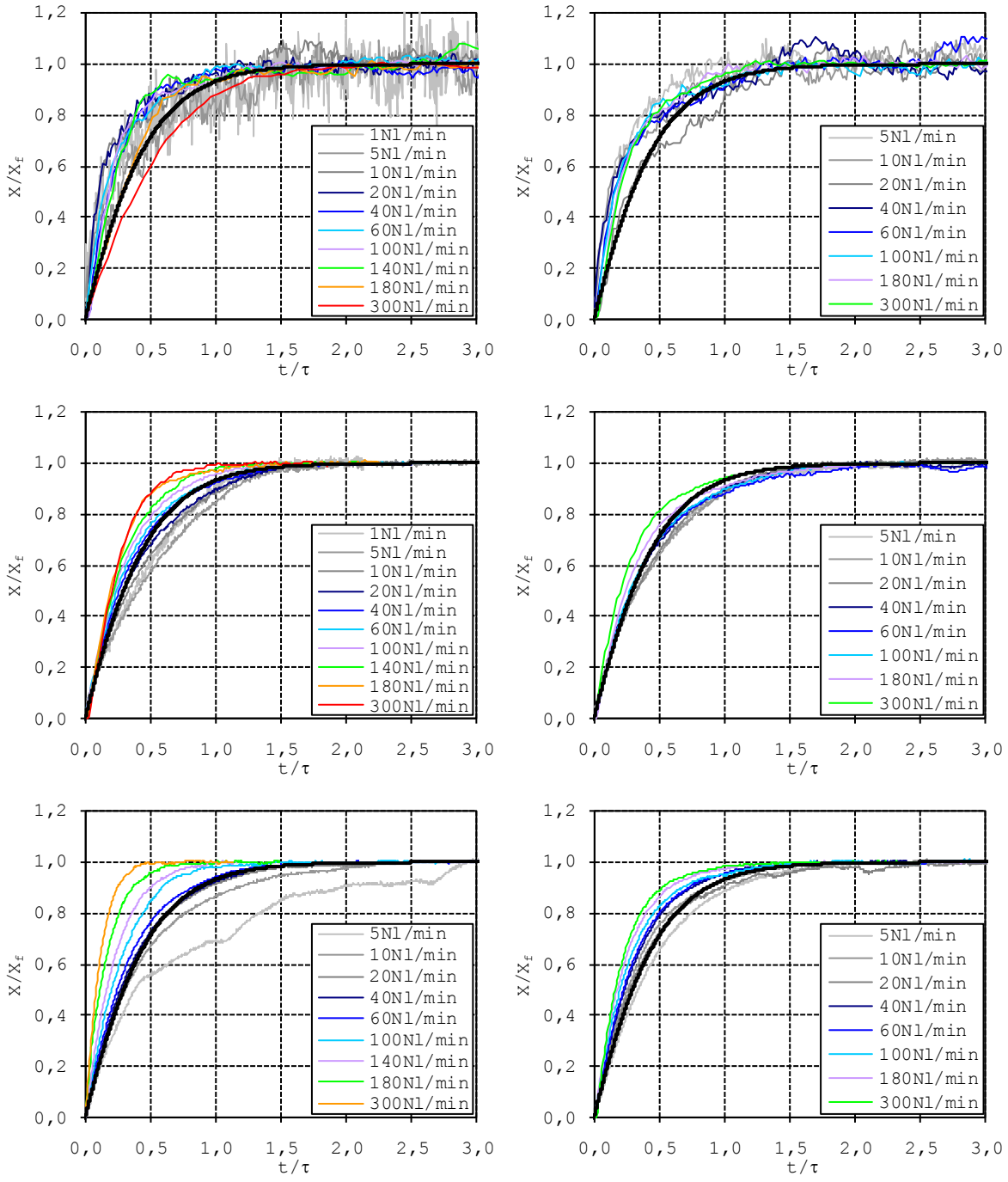

Figure 6 : Temporal evolution of the spatial average helium volume fraction normalized by the steady state value with the 5mm source (left column) and 20mm source (write column), for each vent (a), (b) and (c) from the top to the bottom. The normalization characteristic time is given be eq.(10). The thick black curve results from the integration of eq.(8).

With the vent (a) and the 5mm source, the deviations of results from the model show no clear trend. For larger values of the volume Richardson number corresponding to rates less than 5Nl/min, the results are very noisy because of the very low volume fraction and therefore difficult to interpret. For intermediate volume Richardson numbers from 0.004 to 0.2 (from 140 to 20Nl/min) transients are very close and all faster than the model. In contrast, for the lowest values of the volume Richardson number (0.0008 at 300Nl/min), the transient is slower. With the source of 20mm diameter, almost all the results overlap quite well, and provide a faster transient than the model.

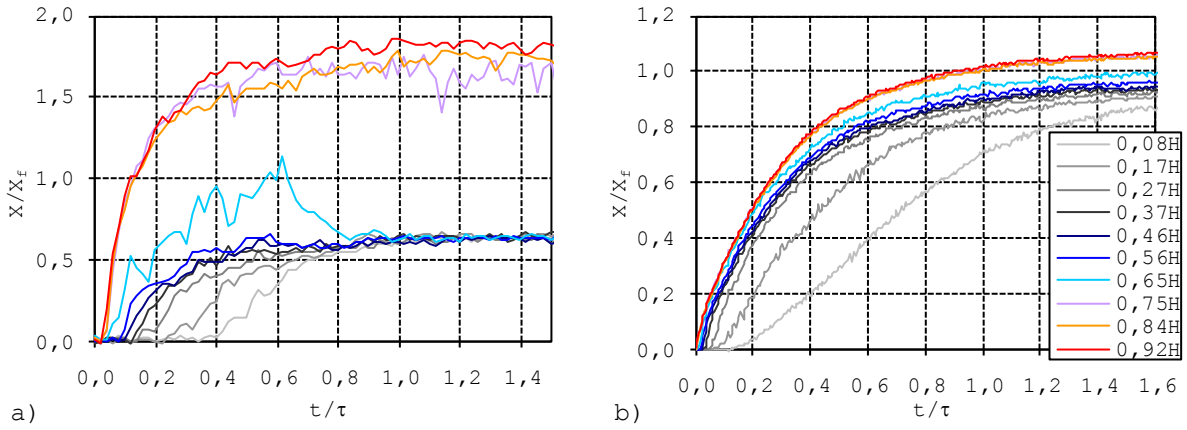

Figure 7: Temporal evolution of the local helium volume fraction with the 5mm source at 40Nl/min; a) with vent (a) and b) with vent (c).

In all cases of injection with the vent (a), it is difficult to correlate these observations with the volume Richardson number variations.

With the vent (b), transients overlap fairly well for volume Richardson number greater than 0.7 (5mm source with a flow rate lower than 10Nl/min or 20mm source with a flow rate lower than 100Nl/min). In these cases, the transient time is slightly longer than that given by the model. Below this value of 0.7 for the volume Richardson number, the transient time has a tendency to decrease for decreasing volume Richardson number. This tendency of decreasing transient time with the volume Richardson number is particularly clear on the results with vent (c).

The local time evolution of the helium volume fraction is detailed for two characteristics experiments with vents (a) and (c). Both are obtained with the 5mm source at a flow rate of 40Nl/min. Fig. 7a shows for vent (a) the settlement of the homogeneous layer near the ceiling as soon as the injection begin. In the lower part, stratification begins to form gradually in a manner quite similar to what can be observed in the absence of natural ventilation. Then there is a homogenization phase which begins approximately at 0.5τ and ends at τ. It is probably the signature of the recirculation motion that may be established in the chamber because of incoming air. These observations also stand for the results with vent (b) but the homogenization is not that clear. The volume fraction local variations for vent (c) are clearly different. It increases gradually at the same rate over the height of the enclosure, producing stratification from the beginning of the injection.

From these observations during the transient we may consider a possible mechanism to explain the steady state vertical distribution observed with vents (a) and (b), *i.e.* close to a two-layer stratification. Instantaneous helium volume fraction profiles corresponding to Fig.7a are shown in Fig. 8a. It clearly shows the rapid formation of a homogeneous layer near the ceiling while there is almost no helium below. This produces an area of strong volume fraction gradient between 0.55H and 0.75H. Then, the volume fraction of helium increases progressively in the lower part. The volume fraction in this area is first stratified until 0.4τ then homogenization occurs during the next 0.4τ, so that eventually the distribution exhibit two homogeneous areas separated by a high gradient. Throughout the transition we note that the gradient in the junction area is increasing.

The helium volume fraction variations are related to density variations of the mixture. In the high density gradient area, buoyancy has a stabilizing effect which acts against vertical motion. The incoming fresh air kinetic energy is not enough to overcome the stabilizing effect of buoyancy of the density gradient, thus leaving the upper part almost unperturbed. This is particularly visible on the time variations shown on Fig. 7a where the volume fraction recorded on the three highest sensors follow a regular increase while below the signals shows some strong variations. Homogenization due to incoming fresh air is only possible in the lower part where the density stratification is weaker.

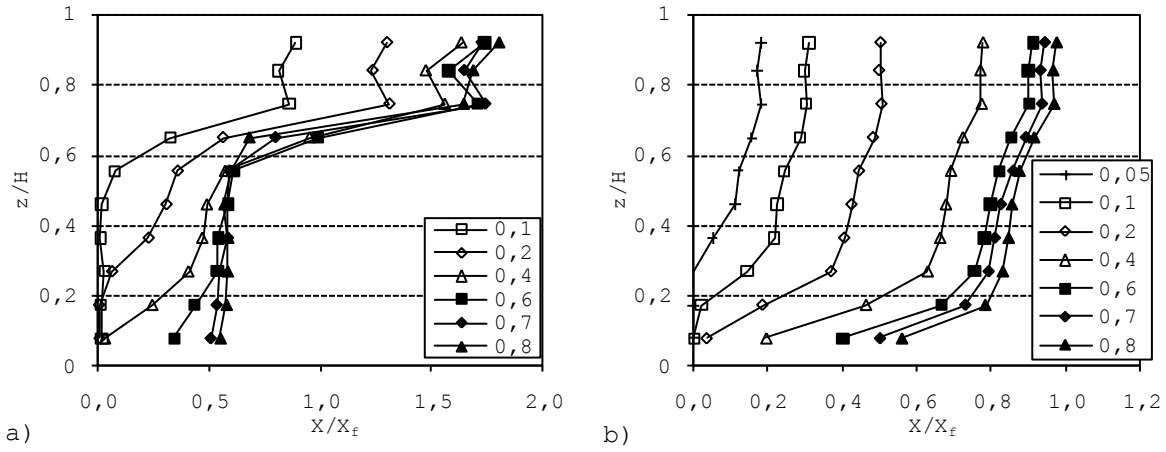

Figure 8 : Instantaneous vertical volume fraction profiles with the 5mm source at 40Nl/min; a) with vent (a) and b) with vent (c). The legend gives the normalized time.

In contrast, with vent (c), there is no formation of such a strong gradient (see Fig. 8b) and stratification sets progressively from the beginning until the steady state. It seems that there is no more recirculation of the fresh air and thus no homogenization over any height. Only a dilution of the mixture occurs near the floor.

From this, it is clear that the geometry of the vent plays a crucial role on the way helium is dispersed vertically. In particular, it seems that a significant vertical size of the opening can promote the formation of a homogeneous layer as soon as the injection begins. Then, this layer determines all the concentration build-up process until the steady state.

5. CONCLUSION

Experiments on the dispersion of a helium jet in an enclosure equipped with a vent have been conducted to assess the effects of its geometry on the spatial and temporal variation of the volume fraction. Injections cover a wide range of volume Richardson number which provides an estimation of the influence buoyant effects compared to momentum effects on the dispersion in the enclosure.

The results obtained for large values of the volume Richardson number show strong vertical variability of the helium distribution. In steady state regime, the structure of the volume fraction vertical distribution is characterized by a homogeneous layer in the upper part. The analysis of the transient phase shows that, for the vent of highest vertical extension, a homogeneous upper layer is formed very quickly producing a high density gradient. The later prevents the establishment of a recirculation due to incoming fresh air over the entire height of the enclosure. Only the lower part is homogenized. With the thinnest vent, although a homogeneous layer is still visible near the ceiling, the stratification is formed gradually during the injection and there is no homogenization of the lower part of the enclosure. Entering fresh air mainly dilutes the near bottom area.

When the volume Richardson number becomes small compared to unity, an increase of the homogeneous layer near the ceiling is observed. This increase is visible only for values of the volume Richardson numbers below 0.05, since even for higher value a homogeneous layer is formed anyway. In the limit of very small volume Richardson number, the dispersion is homogeneous over the height of the enclosure. The critical value of the volume Richardson number obtained to reach this regime is precisely the same than without vent (see [5]), *i.e.,* 0.0023. Thus, there is no influence of the vent on this criterion.

The steady state spatial average volume fraction follows well the power law in $Q^{2/3}$ derived from the homogeneous model until a maximum flow rate beyond which we observe in some cases a change in the slope. Because of the vertical stratification in the enclosure the model has the tendency to overestimate the average volume fraction. Since the model is based on a buoyant exchange at the vent, the volume fraction in the upper part of the enclosure is closer to that given by the model than the average value.

When the source volume flow rate increases, the measured volume fraction significantly deviates from the model due pressure effects. These pressure effects arise when the ratio of the source flow rate to the expected flow rate leaving the enclosure only due to gravity effects exceeds 0.3. The effects of pressure can have several origins. First, the section of the vent may be too low given the volume flow rate to evacuate which could be the case even for large values of the volume Richardson number. Second, jet momentum flux may contribute directly to the flow across the vent.

ACKNOWLEDGEMENTS

The authors are grateful to F. Dabbène and E. Studer for fruitful discussions. This work has been supported by French Research National Agency (A.N.R.) through "*Plan d'Action National sur l'Hydrogène et les piles à combustible"* program (project DIMITRHY ANR-08PANH-006).

6. REFERENCES

[1] W. D. Baines and J. S. Turner, *Turbulent buoyant convection from a source in confined region*, J. Fluid Mech., 37 (1969), p.51-80.

[2] A. E. Germeles, *Forced plumes and mixing of liquids in tanks*, J. Fluid Mech., 71 (1969), p.601-623.

[3] R. P. Cleaver, M. R. Marshall and P. F. Linden, *The build-up of concentration within a single enclosed volume following a release of natural gas*, J. Hazardous Mater., 36 (1994), p.209-226.

[4] Gupta S., Brinster J., Studer E. and Tkatschenko I., *Hydrogen related risks within a private garage: concentration measurements in a realistic full scale experimental facility*, Int. J. Hydrogen Energy, 34 (2009), p. 5902-5911.

[5] B. Cariteau and I. Tkatschenko, *Experimental study of the concentration build-up regimes in an enclosure without ventilation*, submitted to ICHS 2011.

[6] B. Cariteau, J. Brinster and I. Tkatschenko, *Experiments on the distribution of concentration during low flow rate release in an enclosure*, Int. J. Hydrogen Energy, 36 (2011), p.2505-2512.

[7] Venetsanos A. G., Papanikolaou E., Cariteau B., Adams P., Bengaouer A., *Hydrogen permeation from CGH2 vehicles in garages : CFD dispersion calculations and experimental validation*, Int. J. Hydrogen Energy, 35 (2010), p.3848-3856.

[8] P. F. Linden, G. F. Lane-Serff and D. A. Smeed, *Emptying filing boxes: the fluid mechanics of natural ventilation*, J. Fluid Mech., 212 (1990), p.309-335.

[9] P. Linden, *The fluid mechanics of natural ventilation*, Annu. Rev. Fluid Mech., 31 (1999) p.201-238.

[10] Swain M. R. and Swain M. N., *Passive ventilation systems for the safe use of hydrogen*, Int. J. Hydrogen Energy, 21 (1996), p.823-835.

[11] Swain R. M., Grillot E. S., Swain M. N., *Experimental verification of a hydrogen risk assessment method*, Chemical Health and Safety, 1999, p.28-32.

[12] Lowesmith B. J., Hankinson G., Spataru C. and Stobbart M., *Gas build-up in a domestic property following releases of methane/hydrogen mixtures*, Int. J. Hydrogen Energy, 34 (2009), p. 5932-5939.

[13] Barley C. D. and Gawlik K., *Buoyancy-driven ventilation of hydrogen from buildings: laboratory test and model validation*, Int. J. Hydrogen Energy, 34 (2009) , p.5592-5603.

[14] Venetsanos A. G., Papanikolaou E. and Bartzis J. G., *The ADREA-HF CFD code for consequence assessment of hydrogen application*, Int. J. Hydrogen Energy, 35 (2010), p.3908-3918.